Available online at www.sciencedirect.com
SCIENCE DIRECT
Magnetic Resonance Imaging 24 (2006) 295–299
MAGNETIC RESONANCE IMAGING

$T_{1\rho}$ Dispersion profile of rat tissues in vitro at very low locking fields

Seppo K. Koskinen*, Pekka T. Niemi, Sami A. Kajander, Markku E.S. Komu

Department of Diagnostic Radiology, Turku University Hospital, FIN-20520 Turku, Finland

Received 7 April 2005; accepted 11 December 2005

Abstract

The purpose of this study was to show the $T_{1\rho}$ dispersion profile in various rat tissues (liver, brain, spleen, kidney, heart and skeletal muscle) at low (0.1 T) B_0 field at very low locking field B_1, starting from 10 μT. The $T_{1\rho}$ dispersion profile showed a quite similar pattern in all tissues. The highest $R_{1\rho}$ relaxation rates were seen in the liver and muscle followed by the heart, whereas the values for spleen, kidney and brain were rather similar. The greatest difference between R_2 relaxation rate and $R_{1\rho}$ relaxation rate at $B_1=10$ μT was seen in the liver and muscle. The steepest slope for a dispersion curve was seen in the muscle. The value of $T_{1\rho}$ approximately approached the value of T_2 when the locking field B_1 approached 0. Except for the liver, the calculated apparent relaxation rate R'_2 was slightly larger than the calculated one. The potential value of $T_{1\rho}$ imaging is to combine high R_1 contrast of low-field imaging with the high signal-to-noise ratio (SNR) of high static field imaging. $T_{1\rho}$ relaxation and dispersion data presented in the current study help to optimize the rotating-frame MR imaging.

Keywords: $T_{1\rho}$; MRI; Spin lock

1. Introduction

There is as yet no general agreement concerning the complex issue of water relaxation in tissue. However, it can be argued that tissue water protons are relaxed predominantly during the time that they are bound at the protein–water interfaces of cytoplasmic protein [1–5]. This relaxation is greatly enhanced by the fact that cytoplasmic protein is highly organized spatially so that the thermal (Brownian) rotational motion of individual protein molecules is highly restricted [1]. The on–off binding of water molecules causes magnetic field fluctuations, characterized by correlation time, i.e., residence time of the bound water molecule. Also, if water molecules could bind to a large molecule and remain there long enough to sense its relatively slow rotational motion, the proton relaxation of this molecule (at low fields) would be increased 10^6-fold during the period that it remained attached [6]. It can be hypothesized that MR imaging at low magnetic fields would be preferable because relaxation parameters such as longitudinal and transverse relaxation rate ($R_1=1/T_1$ and $R_2=1/T_2$, respectively) reflect the low-frequency components associated with the macromolecules. Also, it has been shown that R_1 at low fields is more tissue specific than at high fields [3]. However, clinical imaging at very low B_0 fields has been impractical because of poor signal-to-noise ratio (SNR).

The longitudinal rotating-frame relaxation time $T_{1\rho}$ [spin-lock (SL)] imaging is an interesting method for investigating slow-motion interactions that cause relaxation [6,7], and $T_{1\rho}$ imaging contrast has been studied in human breast [8], brain [9–11], muscle [12], liver [13], head and neck tumors [14]. It was shown that $T_{1\rho}$ provided improved delineation of breast tumors [8] and showed potential in distinguishing hemangiomas from metastatic liver lesions [13] and benign from malignant head and neck tumors [14]. Also, the longitudinal rotating-frame relaxation rate $R_{1\rho}$ contrast between muscle and fat was found to be clearly higher than R_2 contrast in myositis patients and in healthy volunteers [15]. It has been shown that it is even possible to add $T_{1\rho}$ weighting to a conventional turbo field-echo cine MR sequence to improve the contrast between acutely infarcted and noninfarcted myocardium [16].

A multislice SL pulse sequence can also be implemented on a clinical 1.5-T MR imager for volumetric coverage of an entire anatomic object [17]. Spin-lock imaging has also been shown to be sensitive to changes in proteoglycan content [18,19], and this method has been used to evaluate the

* Corresponding author. Department of Diagnostic Radiology, Töölö Hospital, Helsinki University Central Hospital, 00260 Helsinki, Finland. Tel.: +358 50 4271315; fax: +358 50 41787348.
E-mail address: seppo.koskinen@helsinki.fi (S.K. Koskinen).

0730-725X/$ – see front matter © 2006 Elsevier Inc. All rights reserved.
doi:10.1016/j.mri.2005.04.011

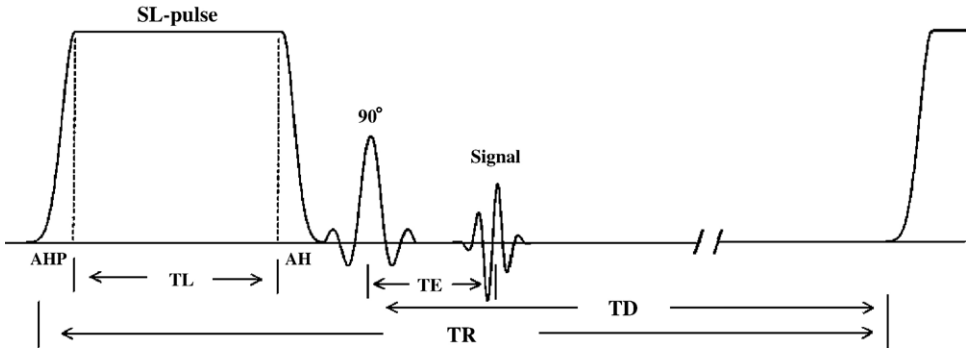

Fig. 1. Spin-locking rf pulse sequence. During the first adiabatic half passage (AHP), the magnetization is locked in the $x'y'$-plane, and after the spin-locking period TL, the magnetization is returned to the direction of the field B_0. The gradient field echo signal is induced at TE from the 90° rf pulse. The next locking pulse starts after the constant TD from the rf pulse.

cartilage in the knee [17,20–23] and wrist [24]. The clear advantage in $T_{1\rho}$ imaging was seen in better SNR when compared to T_2-weighted fat-saturated multi-echo spin-echo sequence [24]. Also, $T_{1\rho}$ is shown to increase in symptomatic osteoarthritic patients when compared to asymptomatic ones [23]. The paramagnetic contrast medium and 3D SL MR imaging can improve the contrast of human gliomas at low field [11]. On post-contrast images, SL imaging significantly enhanced tumor contrast. This method may offer a new modality for tissue characterization improvement of brain tumors.

It has been shown that tissue contrast properties of $R_{1\rho}$ and R_2 are very similar [10,25]. Theoretically, it could be expected that $R_{1\rho}$ would share the tissue characterization qualities of low-B_0-field R_1 as well. In clinical MR imaging, however, the equivalence of $R_{1\rho}$ and R_1 at low B_0 field is more difficult to show, because of the limited clinical data at low B_0 fields. In our earlier works, we focused on $T_{1\rho}$ imaging of protein solutions and muscle tissue [15,25,26] and compared the $R_{1\rho}$ data to previous R_1 data and magnetization transfer of rat tissues at low (0.1 T) B_0 field with locking fields $\geq$50 μT [27]. The aim of the current study was to further exploit the potential of SL imaging and to demonstrate $T_{1\rho}$ dispersion profile in various rat tissues at very low locking fields (<50 μT).

2. Material and methods

2.1. Sample preparations

Five male Sprague-Dawley rats (mean 337 g) were euthanized by means of carbon dioxide asphyxiation. Whole-organ tissue samples included spleen, kidney and heart. Also, excised samples of liver, brain and paraspinal skeletal muscle were included. Five samples of each tissue were harvested. Since $T_{1\rho}$ dispersion of subcutaneous fat was measured earlier (no conspicuous dispersion) [25], it was not included in this study. Superficial blood was removed with tissue paper. Tissue samples were stored in airtight tubes to prevent evaporation, and subsequent, simultaneous MR imaging of all samples was performed at 22.5°C. The imaging part of the experiment took 3 h 30 min. Some change in T_2 but not in T_1 or $T_{1\rho}$ relaxation time has been reported to occur during this time period [28,29].

Sample preparation was similar as in previous study [27].

The experiment was approved by the regional ethical committee for animal research.

2.2. MR imaging

MR imaging was performed on a 0.1-T resistive magnet imager (Merit, Picker Nordstar, Helsinki, Finland) using a double-saddle transmit–receive head coil with quadrature detection. The proper plane was imaged with 20 mm slice thickness and 256×256 data acquisition matrix.

The laboratory frame spin lattice relaxation time T_1 had been obtained earlier with similar tissue specimens in identical conditions [30]. T_2 relaxation time was measured first using a standard spin-echo (repeated single echo) sequence, TR=1500 ms/TE (TE=40–150 ms, a total of 10 different echo times).

The on-resonance rotating-frame relaxation time $T_{1\rho}$ was measured with a SL technique applied to a low-field MR imager [9,12,13]. The SL sequence (Fig. 1) starts with an adiabatic half-passage section of the SL pulse [12,26]. The on-resonance locking rf field B_1 locks the magnetization in the $x'y'$-plane, and the magnetization relaxes during the locking period (TL) with the Zeeman relaxation time $T_{1\rho}$. At the end of the locking pulse, the magnetization is returned to the direction of the external field B_0 with another adiabatic half-passage section. The MR data are collected using a standard gradient echo sequence with a 90° rf pulse immediately after the locking pulse. The next locking pulse starts after a time delay (TD) from the rf pulse. If $BL' < B_1$, where BL' is the local field in the rotating frame, the longitudinal magnetization after the locking pulse produces a relative signal S(TD,TE,TL) at the echo time (TE):

$$S(\mathrm{TE},\mathrm{TD},\mathrm{TL}) = M_0 e^{-\mathrm{TE}/T_2}\left[1 - e^{-\mathrm{TD}/T_1}\right]e^{-\mathrm{TL}/T_{1\rho}} \qquad (1)$$

where M_0 is the equilibrium magnetization, and T_2 and T_1 are the laboratory frame relaxation times at the polarizing field B_0. $T_{1\rho}$ can be determined by measuring the signal